Conference Paper

Investigation of the Wear Resistance Properties of Cr/CrN Multilayer Coatings against Sand Erosion

Muhammad Naveed, Aleksei Obrosov, and Sabine Weiß

Chair of Materials and Physical Metallurgy, Brandenburg Technical University, Konrad Wachsmann Allee 17, 03046 Cottbus, Germany

Correspondence should be addressed to Muhammad Naveed; naveemuh@tu-cottbus.de

This Conference Paper is based on a presentation given by Muhammad Naveed at "European Symposium on Friction, Wear, and Wear Protection" held from 6 May 2014 to 8 May 2014 in Karlsruhe, Germany.

The wear of metallic components used in gas and steam turbines due to erosive sand particles leads to a tremendous decrease in their lifetime. This wear can be reduced by the use of suitable erosion resistant coatings resulting in lower maintenance costs. In this context, multilayer Cr/CrN PVD coatings using an industrial coater were designed and applied on Inconel 718, a material which finds its application in gas turbines. A variation in the bimodal period has been induced in order to achieve an optimal coating architecture providing optimum properties needed for the erosion resistant coatings. The coating was deposited using a single Cr-target with an induction of N_2 during the nitriding phase at a temperature of 480–500°C and the coating thickness of 24–26 μm was kept constant throughout. The erosion tests were conducted at angles of 30°, 60°, and 90°. The sand used for the test is an irregular shaped SiO_2. The erosion tests were followed by a detailed microscopic examination of the eroded coating structure in combination with nanoindentation and scratch tests.

1. Introduction

Solid particle erosion has been identified as a key problem which is responsible for the material removal of blades in aircraft engines operating in dust intensive environments [1]. Historical facts identify erosion as a critical issue as many of the engines had to be replaced after only 20 h during operations in the Gulf-war [2]. Loss of engine performance and reduced mean-time-between overhauls increase in logistic support are some of the problems due to particle erosion of metal components [3]. Hence, coating of metal components for improvement in engine lifetime as well as stable behavior of engines during operation is found to be a possible solution against erosion [4]. The use of single layer nitride coatings (TiN) has been a famous method for protection against erosion due to their high hardness [5, 6]. In contrast, TiAlN coatings with comparatively higher hardness have been devised as a better alternative to TiN coatings [7, 8]. Grögler et al. [9] introduced the use of CVD deposited diamond single layer coatings using low methane (CH_4) content against particle erosion.

A metal-ceramic multilayer architecture is a commonly used coating system, which utilizes the high hardness of the ceramic coating and high fracture toughness of the metal layer. Use of multilayer ceramic-metallic coatings like Ti/TiN [10, 11], W/WN [12], Ti/TiB$_2$ [13], and TiAlN-X (Ti, Al, Cu) [8] has been previously studied in literature. Erosion rater of multilayer coatings was found to be much lower than for single layer coatings [12, 14].

In this paper, a similar approach has been made to understand the wear behavior of metal-ceramic (Cr/CrN) multilayer coatings with various coating architectures. Cr und CrN have been used as a combination of multilayers as they are known for their high adhesion, corrosion, and wear resistance and for their high fracture toughness [15–17]. The present investigation aims to give an insight to the individual critical thickness of metal and ceramic layers required for an optimal coating design, role of the mechanical properties in designing an erosion resistant coating and the crack propagation behavior in various designed coatings. Investigations on the wear behavior due to particle impact
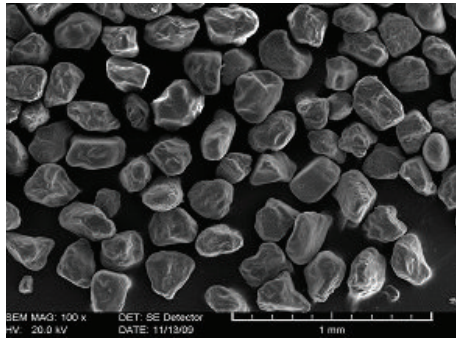
FIGURE 1: SEM image of the erodent used for erosion testing.

FIGURE 2: Coating structure of multilayer Cr1/CrN3 also showing coating growth of Cr and CrN single layer coatings.

can be found in literature [18] and has not been added in this study.

2. Experimental Procedures

2.1. Erosion Test. The erosion tests have been performed on an erosion-test rig. This facility is an in-house build apparatus and consists of a particle feeder, particle injector, acceleration tube, test section, and a compressor. Abrasive particles are filled into the flask of the particle feeder and are fed in a controlled quantity to the particle injector. The abrasive particles are mixed with high pressure air coming from the compressor and the mixture is then accelerated through the acceleration tube. The velocity of the particle can be controlled by adjusting the pressure of the working gas. The accelerated particles are then impacted with a controlled velocity impact on the specimen surface in the test section.

A gravimetric analysis has been performed in order to measure the erosion behavior of coatings at various angles. An in-house designed specimen holder is used for the experiments, which allows to adjust the angles between acceleration tube and specimen. Two specimen have been tested per coating in order to understand the reproducibility of the coatings systems. Tests were performed for incidence angles of 30°, 60°, and 90°.

SiO_2 sand with a particle size range of 75–310 μm was used for the experiments. The sand particles are irregular and sharp-edged with a hardness of 6 Mohs (Figure 1). They are fed with a flow rate of 1 g/min and an average velocity of 75 m/s was measured by means of a laser doppler anemometer (LDA).

2.2. Coating Deposition. The IN-718 specimens with a thickness of 3 mm were cut into 30 × 30 mm coupons. They were than mechanically mirror polished and subjected to chemical and ultrasonic cleaning. Multilayer coatings were then deposited on this specimen in an industrial size PVD-coater HPPMS CC800/9 from CemeCon AG. The target and substrate distance was approximately 70 mm. Prior to the coating deposition process, the specimen were etched using argon gas. This etching process was performed using under vacuum at a pressure of 350 mPa for 30 min.
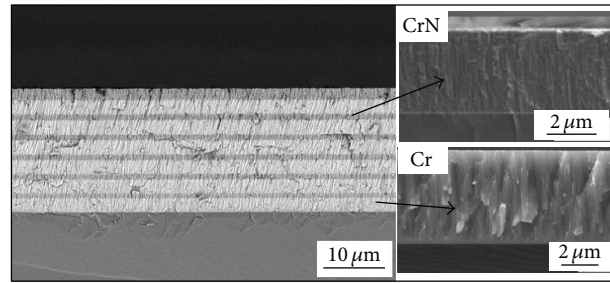
The coatings were deposited in a static mode using a single 99.99% pure Cr target. Alternate Cr and CrN coatings were deposited by controlling the nitrogen flow within a chamber. A flow rate of 40 mln was used for the N_2 gas during the deposition of CrN layer. The coatings were deposited at a temperature range of 480–510°C. The Cr and CrN layers were deposited at a pressure of 300 mPa and a substrate bias of 90 V. A layer of Cr was selected as a first depositing layer in all cases due to its better adhesion with IN-718 substrate. The cathode power of 2000 W was used for both layers, whereas a substrate radio frequency of 110 kHz for Cr and 280 kHz for CrN layer was used in order to improve the adhesion of the coating. The deposition rate for Cr was found 0,15 μm/min and for CrN 0,1 μm/min. Film thickness was measured using a Calowear Test.

2.3. Adhesion and Mechanical Properties. A CSM Instrument Revetest scratch tester was used to investigate the adhesion between the coating layer and the substrate and the critical load. A Berkovich Indenter with a 200 μm in radius was drawn across the coatings surface under increasing normal load. The load was increased gradually starting from 1 to 80 N in an attempt to determine the critical load (L_C) at which a failure occurs. The reported critical load values represent average values of three measurements, which were performed under identical experimental conditions. The scratch tracks on the films were examined by using an optical microscope.

The hardness and E-Modulus measurements have been performed by using a nanoindenter (ASMEC GmbH). The Quasicontinuous Stiffness Method (QCSM) was applied using a Berkovich indenter using and a load of 100 mN. Load-displacement curves have been analyzed in order to obtain the hardness and E-Modulus values of the various coatings. Microscopic investigation has been performed by means of a scanning electron microscope (SEM, Tescan Mira) and an energy dispersive X-ray (EDX) system (OXFORD Instruments).

3. Results and Discussions

3.1. Microstructure. An example of Cr/CrN multilayer coating can be observed in Figure 2. An alternate Cr layer with a thickness of 2,8 μm and CrN layer with a thickness of 1,1 μm is shown in the coating architecture. The coating grew in

TABLE 1: Mechanical properties of single layer Cr, CrN, and multilayer Cr/CrN coatings.

Coating	Bilayer Period (μm)	Total number of layers	Thickness of coating (μm)	Hardness (GPa)	E-Modulus (GPa)	H^3/E^2 (GPa)
Cr	—	1	2.3	7.55 ± 0.43	308.17 ± 22.24	0.214
CrN	—	1	2.1	20.43 ± 1.70	195.76 ± 25.17	0.22
Cr3/CrN1	4	6	24	17.02 ± 1.37	282.92 ± 24.54	0.061
Cr1/CrN3	4	6	24	12.40 ± 1.13	91.80 ± 7.69	0.226
Cr0.25/CrN3.75	4	6	24	21.42 ± 2.18	303.68 ± 30.83	0.106
Cr1/CrN1	2	24	24	20.49 ± 0.86	319.04 ± 14.93	0.084
Cr0.5/CrN0.5	1	48	24	20.05 ± 1.86	252.97 ± 23.73	0.125
Cr0.25/CrN0.25	0,5	96	24	19.82 ± 1.55	298.01 ± 24.04	0.087

form of densely packed columns and is free from cracks and pores. In case of Cr layers, a perpendicular columnar growth of the coating with respect to substrate is observed which tends to orient itself at an angle during the coating growth. Moreover, thin CrN coating finds its growth in accordance to the Cr coating as no discontinuities are observed at the interface of Cr-CrN coating. An individual coating structure of single layer Cr and CrN coatings deposited on single crystal Si-wafer can also be observed in Figure 2. It can be observed that both coatings shown are columnar structure, with Cr columns of larger diameter and porous structure as compare to CrN coatings. This in turn affects the mechanical properties of the coatings, which is discussed in next section.

3.2. Coating Architectures and Mechanical Properties. In order to understand the effect of bimodal period in multilayer coatings, six coatings architectures have been deposited by varying the thickness of metallic and ceramic layer. The total thickness of the coating was always kept constant to a value of 22–26 μm. The individual layer thickness corresponds to the index of the coating given in Table 1.

Hardness and E-Modulus measurements have been performed with a nanoindenter using a load of 10 mN for single layer coatings and 100 mN for multilayer coatings. A 1/10th rule has been followed during the indentation experiments in order to avoid substrate effects. The mechanical properties of the coatings are included in Table 1.

A variation in the mechanical properties of the multilayer coatings was observed due to the change in the thickness of metallic and ceramic layers as low E-Modulus values have been observed for Cr1/CrN3 coating and high E-Modulus for other multilayer systems. A possible reason for low elastic modulus and low hardness of Cr1/CrN3 coatings can be the evolution of a different microstructure and low residual stresses in comparison to other coating architectures which directly influence the mechanical properties of the coatings [19]. With further increase of ceramic layer thickness, the hardness as well as the E-Modulus increased rapidly. This indicates that a critical thickness of ceramic and metal layers has to be achieved in order to achieve high H^3/E^2 ratios. Exceeding the critical thickness values can result in worsening of the mechanical properties of the coatings.

TABLE 2: Adhesion analysis of Cr/CrN coatings deposited on Inconel 718 substrate.

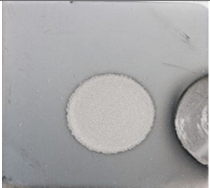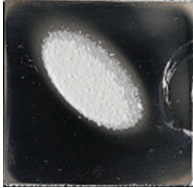| Coating	Adhesion (Lc_2) N
Cr1/CrN1	51.27 ± 3.26
Cr3/CrN1	No results observed
Cr1/CrN3	45.31 ± 3.87
Cr0.25/CrN3.75	18.58 ± 1.11
Cr0.5/CrN0.5	51.35 ± 1.67
Cr0.25/CrN0.25	75.1 ± 1.38

It can also be observed that the H^3/E^2 ratio of CrN coatings is comparable to that of Cr1/CrN3. This behavior is attributed to the thickness and grain size of the Cr layer deposited in the multilayer matrix, affecting the mechanical properties of the multilayer coating [20].

3.3. Coating Adhesion. Scratch tests have been performed in order to evaluate the adhesion of the coatings to the IN718 substrate. For this purpose a progressive loading method with a minimum load of 1 N and a maximum load of 80 N was applied. The results have been evaluated using acoustic emission and depth penetration curves. An average of three critical load values is given in Table 2.

The highest adhesion values were obtained for Cr0.25/CrN0.25 coating whereas Cr0.25/CrN3.75 showed the lowest critical load values. It can be clearly identified that adhesion of coatings with a ceramic layer thickness up to 3 μm showed high to medium critical load values. An increase in thickness of ceramic layer to 3.75 μm results in a rapid decrease of the critical values. Exceeding these critical thicknesses of metal or ceramic layer in a coating architecture influences the mechanical properties of the coating system significantly.

For Cr3/CrN1 coating with a higher amount of metal than ceramic, no clear critical load values have been found for the system. The adhesion test is a method especially for the adhesion evaluation of ceramic coatings. Due to the more metallic character of Cr3/CrN1 no disruption in acoustic emissions indicating spalling of coatings could be observed for this coating.

TABLE 3: Images of the eroded surfaces at various angles.

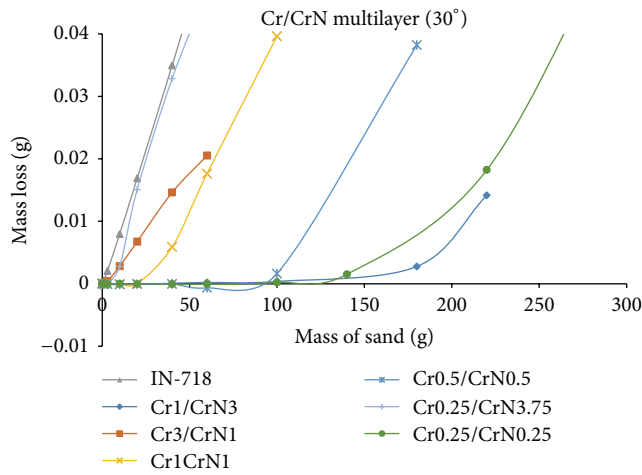| Coatings/angles	30°	60°	90°
Cr0.25/CrN3.75			
Cr0.25/CrN0.25			

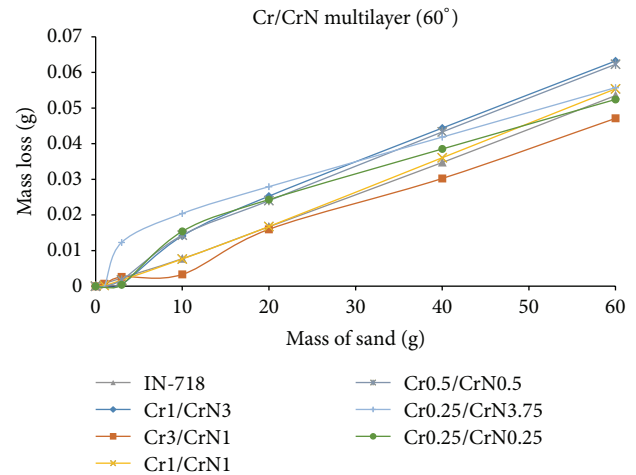FIGURE 3: Mass loss observed during erosion of multilayer Cr/CrN coatings at an incidence angle of 30°.

FIGURE 4: Mass loss observed during erosion of multilayer Cr/CrN coatings at an incidence angle of 60°.

3.4. Gravimetric Analysis. The gravimetric measurements were performed in intervals of 10 g sand for a total amount of 60 g sand. Some specimens, which showed an incubation period for 60 g of sand were further eroded in order to study the erosion mechanism in these coatings. Macroscopic images of the surfaces after erosion at an impact angle of 30°, 60°, and 90° can be observed in Table 3.

It can be observed in Figure 2 that the erosion scar transforms from an elliptical form to a circular shape as the incidence angle is changed from 30° to 90°. The reason for such a transformation is the large contact area eroded by the incidence particles at oblique angles then at normal angles. By comparing the size of the erosion scars of Cr0.25/CrN3.75 and Cr0.25/CrN0.25 at 30° incidence angle, a smaller eroded area is observed for Cr0.25/CrN0.25 due to high erosion resistance offered by the coating. A detailed gravimetric analysis of erosion at various angles can be observed in Figures 3–5.

An analysis of the mass loss at 30° impact angle can be observed in Figure 3. A comparison between In718 substrate and the tested coatings shows that in all cases
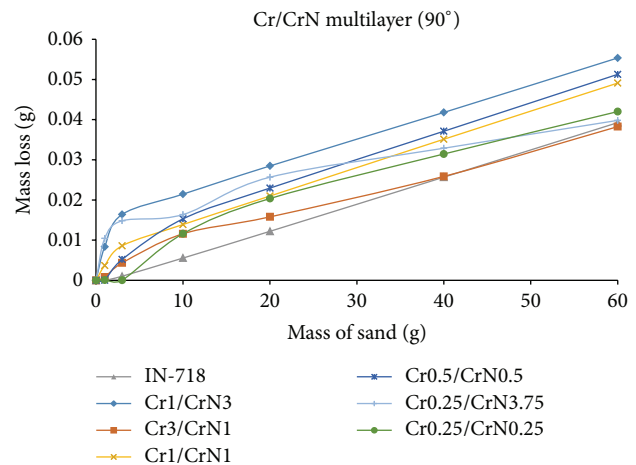

FIGURE 5: Mass loss observed during erosion of multilayer Cr/CrN coatings at an incidence angle of 90°.

the tested coatings were better than substrate without a coating. Cr3/CrN1 and Cr0.25/Cr3.75 showed almost no erosion resistance because material removal takes place without any incubation time. This suggests that the coating structure does not have the capacity to bear the load under these conditions. In contrast, all the other coating systems showed an erosion resistant behavior. The Cr0.25/CrN0.25 and Cr1/CrN3 coatings showed long incubation time of almost 100 minutes. A thin metallic layer (0.25 μm) was probably good enough to withstand external loading but a very thick ceramic layer (3.75 μm) was unable to sustain these loading conditions. In comparison, a relatively thick ceramic layer (3 μm) has high capability to withstand this load. Hence, for a Cr/CrN multilayer coatings, the critical thickness of CrN layer lies between 3 and 3.75 μm seems to be relevant for causing (or inducing) changes in the mechanical behavior.

The mass loss results for an incidence angle of 60° can be seen in Figure 4. None of the coatings showed resistance against erosion. The Cr0.25/CrN0.25 coating reveals a very short incubation period of about 5 minutes (corresponds to 5 g of sand). A parallel course of the curves after first few minutes with an equivalent slope to the one of the uncoated substrate clearly proves that the coating has been removed due to particle erosion in the very first minutes and erosion of the substrate continues.

The mass loss due to erosion at 90° is shown in Figure 5. None of the coatings showed resistance during the erosion process. The highest mass loss was observed for the C1/CrN3 coating. Cr3/CrN1 and Cr0.25/CrN0.25 were the only coatings with a short incubation period during the first few minutes. Hence, the Cr/CrN system is not an effective erosion resistant coating for normal incidence angle. Alegría-Ortega et al. [21] too investigated the erosion behavior of Cr/CrN coatings and found low material loss at 30° compared to at 90°, which was attributed to the brittle behavior of coatings and high material removal due to spallation at normal incident angles.

3.5. Erosion Mechanism. In order to understand the erosion behavior of Cr/CrN multilayer coatings, a number of representative coatings have been chosen to study the crack propagation mechanism in the coating using SEM. A cross-section of the Cr1/CrN3 coating eroded at 30° impact angle is shown in Figure 6(a). In most cases, crack propagation was observed only in the ceramic layer and the crack propagation stops before the metallic layer is reached. This seems to indicate that the toughness of the CrN layer was high enough to prevent the crack from propagating into the metallic layer. Another interesting finding is the direction of crack propagation. Detailed SEM analysis shows that a radial crack formation is supported by the CrN layers which seem to deflect at an angle of approximately 45° within the Cr layer. This difference in crack propagation within metal and ceramic layers results in delayed crack propagation leading to longer incubation time during the erosion.

Figure 6(b) shows a SEM micrograph of the lateral crack propagation in Cr1/CrN1 eroded at an incidence angle of 30°. These lateral cracks probably initiate from the available discontinuities within the coating and find their way parallel to the substrate-coating interface. Most of the lateral cracks observed in the SEM image seem to propagate along the metal-ceramic interfaces in the coating, indicating a week adhesion between the two layers.

PVD coatings grow in form of columnar structures and are prone to failure when these columns are subjected to external loading. Due to impingement of particles with high velocities, bending of these columns take place leading to vertical cracking and shearing of columns [22]. A similar effect can be observed for the Cr1/CrN1 coating eroded at 90° (Figure 6(c)). Once a crack is initiated in the top most layer, instead of crack deflection in the second layer a continuous crack propagation between the grown columns until the crack reaches the substrate is observed. Initiation of lateral cracking is expected in the further stages of the erosion process leading to removal of the coating in form of pieces between two vertical cracks. Failure of coatings due to compressive stresses can be related to the continuous particle impact on the coating surface leading to surface fatigue [23]. Finnie [24] reported on the formation of cone shaped fractures which are related to the ring cracks which intersect in the later phases of erosion process leading to removal of material in large pieces.

The mechanical properties of the substrate also play a vital role in understanding the behavior of the coatings important for the erosion process. Due to high compression loading during the solid particle erosion, the coating applies a compressive stress on the substrate. When these compressive stresses exceed the plastic limit of the substrate, a shear failure of the coating occurs leading to embedding of the coating into the substrate accompanied with substrate deformation (Figure 6(d)). A possible way to reduce this shear failure is to increase the thickness of the coating in order to decrease the intensity of internal stresses between two consecutive layers or between coating and substrate [25].

Another important erosion mechanism, which can be seen in Figure 6(e) for the Cr1/CrN1 multilayer coatings, is the deflection of crack propagation between Cr-CrN layer interface. Once the crack is generated in the top layer, it finds its way to the interface between the metallic and ceramic layer diffusing the stress intensity of the generated crack to penetration in the second layer. This deflection of crack at the interface of a metal-ceramic interface achieved due to elastic modulus mismatch is the advantage of multilayer coatings, which resists the erosion mechanism until complete removal of coating takes place. On the contrary, single layer coatings do not provide reflection of cracks and, hence, crack propagation finds its way through the coatings columns leading to removal of coatings in large pieces [26].

Another important finding was the squeezing of thin CrN between thick metallic Cr layers in Cr3/CrN1 coating system (Figure 6(f)) tested at normal incidence angle. Such a type of behavior can be related to the critical thickness of the layers and the fracture toughness of the coatings. CrN with low thickness and inadequate fracture toughness does not seem to withstand the external loading due to the particles. In contrast, Cr-metallic layers seem to be tough enough to bear the external loading, because no squeezing of metallic layers is observed in the previous discussed cases. Therefore, while designing a multilayer system, it is important
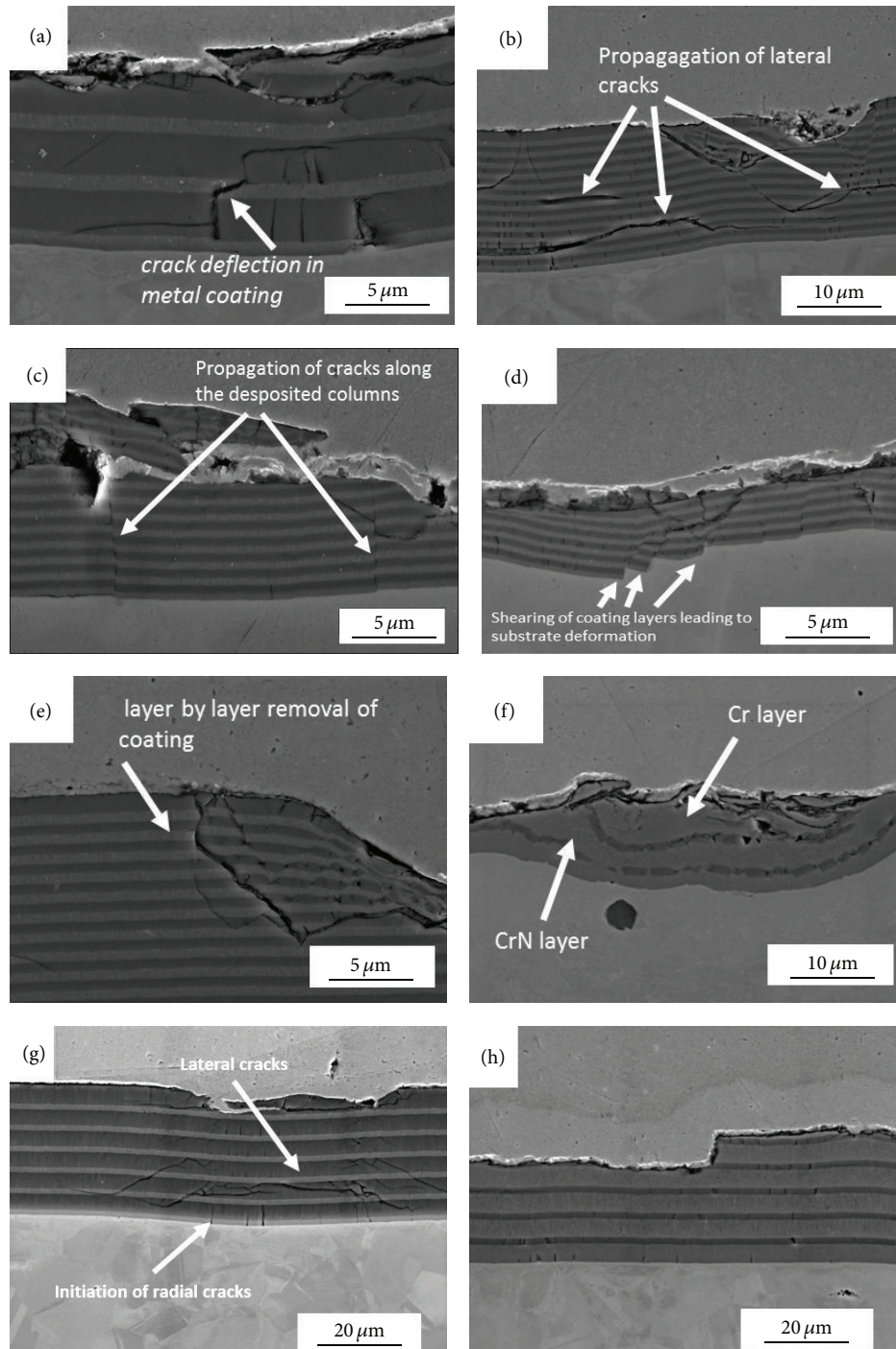
FIGURE 6: SEM images of cross-sections of eroded Cr/CrN coatings (a) Cr1/CrN3@30° (b) Cr1/CrN1@30° (c) Cr1/CrN1@90° (d) Cr0.5/ CrN0.5@90° (e) Cr1/CrN1@30° (f) Cr3/CrN1@90° (g) Cr1/CrN3@60° (h) Cr3/CrN1@60°.

to understand the concept of critical thickness of single layers, so that a combination of mechanical properties can be obtained for the desired applications. SEM and gravimetric analyses of Cr3/CrN1 coating lead to the conclusion that such a system did not provide the advantages of a multilayer coating system where no load bearing capacity of CrN layers were observed in a Cr matrix. Wieciński et al. [27] too reported on the critical thickness of layers where he found

an increase in erosion rate with the increasing ductile phase in Cr/CrN multilayer coating. Maurer and Schulz [22] too discussed the importance of critical thickness of films and postulated a variation in the erosion phenomenon when the coating thickness is sufficiently high or low.

A combination of various wear mechanisms can be observed from the SEM images of Cr1/CrN3 eroded at 60° in Figure 6(g). Interlayer lateral crack propagation observed
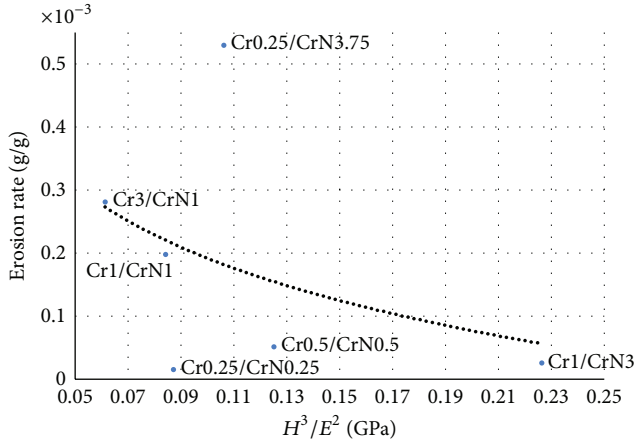
FIGURE 7: Correlation between erosion rate and H^3/E^2 ratio.

generally for shallow incidence angles and origination of radial cracks from the substrate-coating interface typically observed for normal incidence angles can be observed here. Figure 6(h) shows erosion mechanism in Cr3/CrN1 at 60°. It can be seen that some of the coating layers have been broken in form of parts/layers from the coating surface. Such type of behavior is generally not expected from multilayer coatings as a layer to layer removal of material is expected from such a system.

In the literature it was found that thickness ratio of individual layers as well as the bimodal period play an important role to improve tribological properties of coatings [15, 27–29]. Wieciński et al. [27] reported that the thickness ratio of Cr/CrN coatings between 0.65 and 0.81 had the lowest volume loss at oblique angles whereas no erosion resistance was observed in our case. This difference of erosion behavior can be correlated with the difference of coating architectures and the testing conditions applied during erosion tests.

4. Dependence of Erosion on the H^3/E^2 Ratio

Literature identifies various ratios for the description of mechanical parameters like H/E, H^2/E and H^3/E^2 [30] in order to study the erosion resistance of the coating in reference to the material properties. In the present study, a correlation between the coating resistance to the onset of plastic deformation (H^3/E^2) and erosion rate at an incidence angle of 30° can be observed. The erosion rate is defined as

$$\text{Erosion Rate} = \frac{\text{Mass of specimen removed (g)}}{\text{Mass of impacting particles (g)}}. \quad (1)$$

The illustration (Figure 7) shows that a decreasing trend of erosion rate with the increasing H^3/E^2 ratio for all coatings. Two multilayer coatings Cr0.25/CrN3.75 and Cr0.25/CrN0.25 show no direct correlation in this case. By increasing the thickness of CrN coating from 3 to 3.75 μm, the residual tensile stress probably increases in the coating layer, which leads to inadequate resistance against crack propagation [31]. Hence, it is important to determine the

critical thickness of the individual Cr and CrN layers in order to achieve good performance of the coating system.

A possible explanation of the deterioration of the mechanical properties of Cr0.25/CrN0.25 can be the decrease in the bilayer period [32]. Previous investigations show that hardness of multilayer systems increases with increasing bimodal period but a constant or decreased hardness is observed after a critical bimodal period is surpassed [33]. A similar behavior was reported by Marulanda et al. [34] where an increase in wear volume for coatings with a bimodal period of 20 nm was found. The behavior was associated to the weak interface bonding strength and residual stresses present in the coatings [35]. Therefore, it is supposed that a deterioration of the mechanical properties of Cr0.25/CrN0.25 coating can be related to the 96 layers which are a part of the coating architecture. Moreover, residual stresses generally increase with the increase in modulation period [36]; therefore the presence of high residual stresses in the coating can be expected in this case. Stress measurements, planned for the near future, may provide clear statements on the effect of bimodal periods in the multilayer coatings.

According to this study, for a better resistance against solid particle erosion, H^3/E^2 ratios should be maximized by achieving optimal values of hardness (H) and low elastic modulus (E). Such a combination will improve the resistance against plastic deformation and brittle failure.

5. Conclusions

In this study the erosion behavior of metal-ceramic (Cr/CrN) multilayer coatings with various coating architectures was investigated. The following results were obtained.

(1) Erosion resistance of coatings was observed for oblique incidence angles whereas no erosion protection was observed at normal and near normal incidence angle.

(2) The adhesion between the coating and substrate is one of the critical parameters, which defines the erosion behavior of a coating. In this study coatings with higher substrate-coating adhesion showed an optimum erosion resistance whereas coatings with low adhesion were unable to withstand the harsh testing conditions.

(3) The erosion resistance to plastic yield (H^3/E^2) shows a direct correlation with the decreasing erosion rate. Hence, erosion resistance can be improved by achieving high hardness in combination with low E-Modulus values of the multilayer coatings.

(4) It is important to determine the critical thickness of the layers to achieve good performance of the coating system. It was observed that the best erosion resistance was obtained with an individual layer thickness of 3 μm whereas no resistance was observed for a coating thickness of 3.75 μm.

(5) Various erosion mechanisms like lateral cracking, radial cracking, crack deflection at the coating interfaces and, deformation of substrate due to shearing of the coating, all related to the coating architecture, were observed.

Conflict of Interests

The authors declare that there is no conflict of interests regarding the publication of this paper.

References

[1] R. C. Sirs, "The operation of gas turbine engines in hot & sandy conditions-royal air force experiences in the gulf war," Tech. Rep. AGARD-CP-558, Paper no. 2, 1994.

[2] A. Hamed, W. Tabakoff, and R. Wenglarz, "Erosion and deposition in turbomachinery," *Journal of Propulsion and Power*, vol. 22, no. 2, pp. 350–360, 2006.

[3] J. P. van der Walt and A. Nurick, "Erosion of dust-filtered helicopter turbine engines part I: basic theoretical considerations," *Journal of Aircraft*, vol. 32, no. 1, pp. 106–111, 1995.

[4] L. Swadźba, B. Formanek, H. M. Gabriel, P. Liberski, and P. Podolski, "Erosion- and corrosion-resistant coatings for aircraft compressor blades," *Surface and Coatings Technology*, vol. 62, no. 1–3, pp. 486–492, 1993.

[5] A. Feuerstein and A. Kleyman, "Ti-N multilayer systems for compressor airfoil sand erosion protection," *Surface and Coatings Technology*, vol. 204, no. 6-7, pp. 1092–1096, 2009.

[6] S. Hassani, J. E. Klemberg-Sapieha, M. Bielawski, W. Beres, L. Martinu, and M. Balazinski, "Design of hard coating architecture for the optimization of erosion resistance," *Wear*, vol. 265, no. 5-6, pp. 879–887, 2008.

[7] Q. Yang, D. Y. Seo, L. R. Zhao, and X. T. Zeng, "Erosion resistance performance of magnetron sputtering deposited TiAlN coatings," *Surface and Coatings Technology*, vol. 188-189, no. 1–3, pp. 168–173, 2004.

[8] J. M. Castanho and M. T. Vieira, "Effect of ductile layers in mechanical behaviour of TiAlN thin coatings," *Journal of Materials Processing Technology*, vol. 143-144, no. 1, pp. 352–357, 2003.

[9] T. Grögler, E. Zeiler, A. Franz, O. Plewa, S. M. Rosiwal, and R. F. Singer, "Erosion resistance of CVD diamond-coated titanium alloy for aerospace applications," *Surface and Coatings Technology*, vol. 112, no. 1–3, pp. 129–132, 1999.

[10] A. Leyland and A. Matthews, "Thick Ti/TiN multilayered coatings for abrasive and erosive wear resistance," *Surface and Coatings Technology*, vol. 70, no. 1, pp. 19–25, 1994.

[11] B. Borawski, J. Singh, J. A. Todd, and D. E. Wolfe, "Multi-layer coating design architecture for optimum particulate erosion resistance," *Wear*, vol. 271, no. 11-12, pp. 2782–2792, 2011.

[12] Y. Gachon, P. Ienny, A. Forner, G. Farges, M. C. Sainte Catherine, and A. B. Vannes, "Erosion by solid particles of W/W-N multilayer coatings obtained by PVD process," *Surface and Coatings Technology*, vol. 113, no. 1-2, pp. 140–148, 1999.

[13] N. Panich, P. Wangyao, S. Hannongbua, P. Sricharoenchai, and Y. Sun, "Tribological study of nano-multilayered ultra-hard coatings based on TiB2," *Reviews on Advanced Materials Science*, vol. 13, no. 2, pp. 117–124, 2006.

[14] E. Quesnel, Y. Pauleau, P. Monge-Cadet, and M. Brum, "Tungsten and tungsten-carbon PVD multilayered structures as erosion-resistant coatings," *Surface and Coatings Technology*, vol. 62, no. 1-3, pp. 474–479, 1993.

[15] L. Major, J. Morgiel, B. Major et al., "Crystallographic aspects related to advanced tribological multilayers of Cr/CrN and Ti/TiN types produced by pulsed laser deposition (PLD)," *Surface and Coatings Technology*, vol. 200, no. 22-23, pp. 6190–6195, 2006.

[16] A. Lousa, J. Romero, E. Martínez, J. Esteve, F. Montalà, and L. Carreras, "Multilayered chromium/chromium nitride coatings for use in pressure die-casting," *Surface and Coatings Technology*, vol. 146-147, pp. 268–273, 2001.

[17] E. Martinez, J. Romero, A. Lousa, and J. Esteve, "Wear behavior of nanometric CrN/Cr multilayers," *Surface and Coatings Technology*, vol. 163-164, pp. 571–577, 2003.

[18] J. Deng, F. Wu, Y. Lian, Y. Xing, and S. Li, "Erosion wear of CrN, TiN, CrAlN, and TiAlN PVD nitride coatings," *International Journal of Refractory Metals and Hard Materials*, vol. 35, pp. 10–16, 2012.

[19] C. A. Johnson, J. A. Ruud, R. Bruce, and D. Wortman, "Relationships between residual stress, microstructure and mechanical properties of electron beam-physical vapor deposition thermal barrier coatings," *Surface and Coatings Technology*, vol. 108-109, no. 1–3, pp. 80–85, 1998.

[20] P. Wieciński, J. Smolik, H. Garbacz, and K. J. Kurzydłowski, "Failure and deformation mechanisms during indentation in nanostructured Cr/CrN multilayer coatings," *Surface and Coatings Technology*, vol. 240, pp. 23–31, 2014.

[21] J. A. Alegría-Ortega, L. M. Ocampo-Carmona, F. A. Suárez-Bustamante, and J. J. Olaya-Flórez, "Erosion-corrosion wear of Cr/CrN multi-layer coating deposited on AISI-304 stainless steel using the unbalanced magnetron (UBM) sputtering system," *Wear*, vol. 290-291, pp. 149–153, 2012.

[22] C. Maurer and U. Schulz, "Solid particle erosion of thick PVD coatings on CFRP," *Wear*, vol. 317, no. 1-2, pp. 246–253, 2014.

[23] I. M. Hutchings, "Some comments on the theoritical treatment of erosive particle impacts," in *Proceedings of the 5th International Conference on Erosion by Solid and Liquid*, Cambridge University, Cambridge, UK, 1979.

[24] I. Finnie, "Erosion by a stream of solid particles," *Wear*, vol. 2, pp. 111–122, 1967.

[25] C. Maurer and U. Schulz, "Erosion resistant titanium based PVD coatings on CFRP," *Wear*, vol. 302, no. 1-2, pp. 937–945, 2013.

[26] O. Schroeter, "Herstellung und Chrakterisierung von PVD-Schichten auf Basis der Cr2AlC-MAX-Phase," in *Metallkunde und Werkstofftechnik*, Brandenburgische Technische Universität, 2011.

[27] P. Wieciński, J. Smolik, H. Garbacz, and K. J. Kurzydłowski, "Erosion resistance of the nanostructured Cr/CrN multilayer coatings on Ti6Al4V alloy," *Vacuum*, vol. 107, pp. 277–283, 2014.

[28] R. Bayón, A. Igartua, X. Fernández et al., "Corrosion-wear behaviour of PVD Cr/CrN multilayer coatings for gear applications," *Tribology International*, vol. 42, no. 4, pp. 591–599, 2009.

[29] L. Zhang, H. Yang, X. Pang, K. Gao, and A. A. Volinsky, "Microstructure, residual stress, and fracture of sputtered TiN films," *Surface and Coatings Technology*, vol. 224, pp. 120–125, 2013.

[30] S. Hassani, M. Bielawski, W. Beres, L. Martinu, M. Balazinski, and J. E. Klemberg-Sapieha, "Predictive tools for the design of erosion resistant coatings," *Surface and Coatings Technology*, vol. 203, no. 3-4, pp. 204–210, 2008.

[31] C. L. Martin, O. O. Ajayi, S. Torrel, N. Demas, A. Erdemir, and R. Wei, "Effect of coating thickness on tribological performance of CrN in dry sliding contact," in *Proceedings of the ASME/STLE International Joint Tribology Conference*, pp. 75–77, Denver, Colo, USA, October 2012.

[32] M. Kot, W. A. Rakowski, Ł. Major, R. Major, and J. Morgiel, "Effect of bilayer period on properties of Cr/CrN multilayer coatings produced by laser ablation," *Surface and Coatings Technology*, vol. 202, no. 15, pp. 3501–3506, 2008.

[33] J. Romero, A. Lousa, E. Martínez, and J. Esteve, "Nanometric chromium/chromium carbide multilayers for tribological applications," *Surface and Coatings Technology*, vol. 163-164, pp. 392–397, 2003.

[34] D. M. Marulanda, J. J. Olaya, U. Piratoba, A. Mariño, and E. Camps, "The effect of bilayer period and degree of unbalancing on magnetron sputtered Cr/CrN nano-multilayer wear and corrosion," *Thin Solid Films*, vol. 519, no. 6, pp. 1886–1893, 2011.

[35] Y. Zhou, R. Asaki, W.-H. Soe, R. Yamamoto, R. Chen, and A. Iwabuchi, "Hardness anomaly, plastic deformation work and fretting wear properties of polycrystalline TiN/CrN multilayers," *Wear*, vol. 236, no. 1-2, pp. 159–164, 1999.

[36] M. Liu, M. Tan, G. Liu et al., "The effects of modulation period, modulation ratio, and deposition temperature on microstructure and mechanical properties of ZrB_2/W multilayers," *Science China Technological Sciences*, vol. 53, no. 9, pp. 2350–2354, 2010.